



# PARAMETER IDENTIFICATION FOR A ROBOTIC MANIPULATOR ARM

D. W. Brewer  
Institute for Computer Applications in Science and Engineering

and

J. S. Gibson  
University of California, Los Angeles

## Abstract

This paper describes the development of a nonlinear dynamic model for large oscillations of a robotic manipulator arm about a single joint. Optimization routines are formulated and implemented for the identification of electrical and physical parameters from dynamic data taken from an industrial robot arm. Special attention is given to the role of sensitivity in the formulation of robust models of this motion. The importance of actuator effects in the reduction of sensitivity is established and used to develop an electro-mechanical model of the manipulator system.

---

Research was supported by the National Aeronautics and Space Administration under NASA Contract No. NAS1-17070 while the authors were in residence at ICASE, NASA Langley Research Center, Hampton, VA 23665-5225.

## **1. Introduction**

The purpose of this research is to develop and investigate methods for identifying parameters in a dynamic model of a robotic manipulator. Identification routines of this type are important in the construction of control algorithms for manipulator systems [4]. Because the parameter identification must be based on input and output data from an assembled manipulator, which acts under gravity and has possibly complicated joint friction, the dynamic model is a nonlinear differential equation, which must be solved numerically.

The approach used to date is to employ a nonlinear search routine to minimize a quadratic fit-to-data criterion formed using the experimental data and the solution to the model equation. This method has been applied to a Unimation 600 Puma arm, with data obtained by F. W. Harrison in the Intelligent Systems Robotics Laboratory at the NASA Langley Research Center.

Section 2 describes the mathematical model of the manipulator arm and the parameters to be identified. Section 3 describes the parameter identification scheme and the computer algorithms used. In Section 4, the experiment is discussed in more detail, along with some preliminary data reduction and analysis of the relationship between angular velocity and torque. Section 5 presents an analysis of the sensitivity of the manipulator arm model to perturbations of uncertain parameters and initial conditions. We also discuss a method for reducing this sensitivity which in this application corresponds to the inclusion of a back electromotive force in the arm model. In Section 6 we discuss the results of the parameter estimation routines for several models of robot arm friction.

## 2. Manipulator Model

To minimize the number of unknown parameters in each set of data, each experiment was performed with all but one manipulator joint locked. For each experiment, then, the model of the manipulator is a rigid arm that pivots about the one moving joint at a point 0. Thus, the arm in the model for a given experiment consists of several manipulator links, including the end effector, constrained to move as a rigid body. The equation of motion is

$$(2.1) \quad J\ddot{\theta} - mgr\sin\theta + f(\dot{\theta}) = u(t)$$

where  $\theta$  is the angle between the arm and the upward vertical and  $u$  is the control torque applied to the arm by the electric motor (actuator) at the joint in question. The damping term  $f(\dot{\theta})$  represents friction in both the joint and the motor;  $J$  is the moment of inertia about the appropriate joint,  $m$  is the mass of the arm,  $g$  is the acceleration of gravity, and  $r$  is the distance from 0 to the arm's center of mass.

The angle between the arm and the vertical was measured at sampling times  $t_i$  and the sampling rate was 30 Hertz, so that

$$(2.2) \quad t_s = t_{i+1} - t_i = 1/30 \text{ sec.}$$

We will denote this measured angle (i.e., the data) by  $y(t_1)$  to distinguish it from the solution to the model equation (2.1).

The basic idea of the parameter identification scheme is to find parameters for (2.1) so that the solution to this differential equation matches the measured angle as closely as possible at the sampling times.

Because we cannot identify all of the parameters in (2.1) from the experiment described, we must define a minimal set of parameters for this model. Therefore, we rewrite (2.1) as

$$(2.3) \quad \ddot{\theta} - \alpha \sin \theta + f(c_1, c_2, \dot{\theta}) = \beta u(t)$$

where  $\alpha = mgr/J$ ,  $\beta = 1/J$ , and we have parameterized the the damping term  $f(\dot{\theta})$  in (2.1) as  $f(c_1, c_2, \dot{\theta})$ . The damping term  $f(\dot{\theta})$  may include various forms of dissipation: linear damping, nonlinear damping, and Coulomb friction. Our best results have come with (sometimes piecewise) linear damping and quadratic damping in combination with a linear damping term resulting from back electromotive force.

We will refer to the set of parameters in (2.3) by the parameter vector

$$(2.4) \quad \mathbf{q} = [\alpha \ \beta \ c_1 \ c_2 \ \cdot \ \cdot \ \cdot].$$

### 3. Parameter Identification

An experiment performed on a time interval  $[t_0, t_f]$  yields data  $u(t_i)$  and  $y(t_i)$ ,  $t_i = t_0, t_0 + t_s, \dots, t_f$ . With the known command torque  $u(t)$  and a set of trial parameters, we solve (2.3) on the interval  $[t_0, t_f]$  and form the fit-to-data criterion

$$(3.1) \quad J(\mathbf{q}) = \sum [\theta(t_i) - y(t_i)]^2.$$

The parameter identification then consists of finding the parameter vector  $\mathbf{q}$

to minimize  $J(\mathbf{q})$ . Usually, we take the initial time  $t_0 \geq 2$  sec. because we suspect some error in the data near the beginning of the experiment due to transients in electronics. Therefore, in some cases we know that the initial angular velocity is zero, but in most cases we must estimate it using finite differences obtained from the position measurement.

To solve (2.3), we use a fourth-order Runge-Kutta algorithm with variable step size [3]. We tried using the numerical integrators DGEAR and DVERK in the IMSL library, but both of these routines often hung up--i.e., the step size was reduced to zero--where the manipulator arm turned. This was especially troublesome for models with piecewise continuous damping and Coulomb friction. The step-size control in our final Runge-Kutta routine does not allow the step size to fall below a specified minimum.

For minimizing  $J(\mathbf{q})$  we used the subroutine ZXSSQ from the IMSL library, which is a Levenberg-Marquardt algorithm [2] that approximates gradients by finite differences. It also estimates the Hessian. Hence we assume certain smoothness and local convexity of  $J(\mathbf{q})$  and the performance of the algorithm indicates that these assumptions are valid.

#### **4. Data Collection and Analysis**

Experimental data was collected by F. W. Harrison in the Intelligent Systems Robotics Laboratory at NASA Langley Research Center. The subject of the experiments was a UNIMATE PUMA industrial robot with six degrees of freedom. A schematic [1] of the robot arm with rotational joints is shown in Figure 1. The experiments described below were performed by rotating only the shoulder (joint 2) with all other joints locked in a collinear position.

a. Static Experiment

The purpose of this experiment was to establish a relationship between the current delivered to joint 2 and the torque exerted on the robot arm. The arm was placed in a horizontal position and the force exerted by the arm at a fixed distance from the joint was measured at a sequence of motor current levels. The results of this experiment are shown in Figure 2. Because of the linear relationship of these quantities, it was decided to use the measured motor current data as the torque input in our dynamic models of the arm motion.

b. Dynamic Experiment

The purpose of this experiment was to gather input and output data for the dynamic model described in Section 2. The arm was initialized in a vertical, upright position and then commanded to rotate about joint 2 through an angle of approximately 90 degrees in both directions. During this oscillation, 512 measurements of the joint angle in radians and the motor current as measured by the voltage drop across a known resistance were taken at a frequency of 30 Hertz. These input and output data are illustrated in Figures 3 and 4, respectively. The angular velocity of the robot arm, calculated by backward differences, is shown in Figure 5.

c. Command Torque Synthesis

This data analysis is designed to recover the square-wave commanded voltage across the motor terminals. If only back electromotive force is included in the motor model, then this commanded voltage is the sum of the voltage drop across the motor resistance (Figure 3) and the angular velocity (Figure 5) multiplied by the back emf constant. Figure 6 shows the results of

this computation for a back emf constant of 1.5, estimated by trial-and-error. In Section 5 a square-wave approximation of Figure 6 is used as input to an alternate model of the robotic system which includes back emf effects.

### 5. Sensitivity Analysis

In this section we discuss the sensitivity of the solution of the nonlinear model

$$(5.1) \quad \left\{ \begin{array}{l} \ddot{\theta} - \alpha \sin \theta + f(c_1, c_2, \dot{\theta}) = \beta u(t) \\ \theta(0) = \theta_0 \\ \dot{\theta}(0) = \omega_0 \end{array} \right.$$

with respect to small perturbations of the initial velocity  $\omega_0$  and the unknown friction parameter  $c_1$ .

In some applications of parameter estimation, moderately high parameter sensitivity is advantageous in that it allows the unknown parameters to be estimated with a greater degree of certainty for a given level of noise in the output data. However, in parameter estimation for simulation, a sensitive model will yield poor simulations when the unknown parameters are subjected to slight variations due to modeling errors or external factors. For this reason it is preferable to have a mathematical model which is relatively stable with respect to perturbations of the parameters.

The same reasoning applies to perturbations of initial conditions. In this application only the initial position can be measured directly for a selected subinterval of the data. The angular velocity, computed by a finite



difference, is subject to considerable error. Therefore, it is desirable to have a simulation model which is not subject to high sensitivity with respect to this initial condition.

Unfortunately, numerical testing indicates a substantial degree of sensitivity on both parameters and initial conditions for the model (5.1) with measured motor current as input. Figure 7 indicates the effect on the output of a small perturbation of the friction coefficient  $c_1$ , and Figure 8 shows a similar comparison for a small perturbation of the initial velocity  $\omega_0$ . In fact this figure indicates an almost chaotic dependence of this model on the initial angular velocity.

We therefore undertake a mathematical method for reducing this sensitivity which in this application has physical implications as well. The basic idea is to increase the damping in the system by adding a term of the form  $\beta k \dot{\theta}$  to both sides of the differential equation. Setting  $v(t) = u(t) + k \dot{\theta}(t)$  yields

$$(5.2) \quad \ddot{\theta} - \alpha \sin \theta + [f(c_1, c_2, \dot{\theta}) + \beta k \dot{\theta}] = \beta v(t)$$

which is of the same form as (5.1) except that the damping term has been increased at the expense of changing the input function. If, in the parameter estimation procedure, the new input  $v(t)$  can be either measured directly or synthesized from data, then equation (5.2) is a model which may possess greater stability with respect to initial conditions and parameter values. This factor tends to yield numerical solutions for the state which are more reliable over long time intervals and therefore lead to more robust parameter estimates.

A numerical test of this procedure is shown in Figures 9 and 10. These figures show the output of a model based on (5.2). The input  $v$  is the synthesized commanded motor terminal voltage (Figure 6). The damping parameters are greater because they include back emf effects. The numerical results show significantly lower sensitivity on friction parameters (Figure 9) and initial angular velocity (Figure 10).

The physical implications of the mathematical procedure for this system have already been indicated. By using the commanded motor terminal voltage as input rather than the torque delivered to the joint, one arrives at a more stable model of the robot dynamics. In effect, the model which includes back emf takes advantage of a natural damping in the electro-mechanical system. One can obtain good fit-to-data over short time intervals for the mechanical system alone, but the stability provided by this effect is lost.

## 6. Numerical Results

The iterative parameter estimation routine described in Section 3 was applied to the model (5.1) on the time interval [1.67, 15.0]. The results are given in Table 1. Three alternative friction models were employed: linear friction given by

$$(6.1) \quad f(x) = cx,$$

quadratic friction of the form

$$(6.2) \quad f(x) = c_1 x + c_2 x|x|,$$

and piecewise linear, direction-dependent friction model of the form

$$(6.3) \quad f(x) = \begin{cases} c_1 x, & x > 0, \\ c_2 x, & x < 0. \end{cases}$$

As shown in Table 1, the cost function (3.1) is quite large for all three friction models and the iterative method does not converge.

The results of the same procedure for the desensitized model (5.2) with input given in Figure 6 are shown in Table 2. The friction values are larger because they include the effect of back emf. The procedure shows convergence to relatively low cost values for each of the three friction models. The direction-dependent friction model (6.3) shows the most rapid convergence to the lowest cost value. While the quadratic friction model (6.2) eventually obtains a low cost, it converges much more slowly and alters the physical parameters  $\alpha$  and  $\beta$  to values which are quite different from those obtained by models (6.1) and (6.3). The solid graph in Figure 10 show the output of the most accurate model in Table 2. This graph is almost indistinguishable over this time interval from the graph of the measured robot arm motion (Figure 4).

## 7. Conclusion

Our experience indicates the importance of actuator effects in the development of robust dynamic models for the motion of a robotic manipulator arm. The inclusion of natural damping due to back emf effects improved the performance of both the numerical integrator for solving the nonlinear

equation of motion and the numerical optimizer for estimating parameters. Among the friction models we studied, the model allowing direction-dependent damping coefficients was the most successful. In continuing research, we plan to combine this model with a first-order dynamic model of the actuator to study more complex motions of the robotic manipulator arm.

### References

- [1] L. Keith Barker, "Kinematic equations for resolved-rate control of an industrial robot arm," NASA TM-85685, 1983.
- [2] R. Fletcher, Practical Methods of Optimization, Vol. 1, John Wiley and Sons, 1981.
- [3] C. William Gear, Numerical Initial Value Problems in Ordinary Differential Equations, Prentice-Hall, 1971.
- [4] B. K. Kim and K. G. Shin, "Suboptimal control of industrial manipulators with a weighted minimum time-fuel criterion," IEEE Trans. Automatic Control 30 (1985), pp. 1-10.

**Table 1. Numerical Results for Model (5.1).**

---



---

Linear friction model (6.1)					
iterate	$\alpha$	$\beta$	$c$	cost	
0	13.39	21.00	1.17	82300.	
1	16.33	24.07	1.08	65600.	
2	15.51	22.64	1.12	137000.	
3	11.72	13.64	1.18	6110.	
4	13.18	11.58	3.23	5410.	
5	14.14	10.31	4.03	5240.	

Quadratic friction model (6.2)					
iterate	$\alpha$	$\beta$	$c_1$	$c_2$	cost
0	13.39	21.00	1.17	0.00	82300.
1	31.55	38.38	3.13	0.55	152000.
2	26.72	23.31	5.47	0.58	103000.
3	180.4	130.5	27.2	2.96	56800.

Piecewise linear friction model (6.3)					
iterate	$\alpha$	$\beta$	$c_1$	$c_2$	cost
0	12.05	21.42	2.59	4.87	450.
1	11.23	20.73	3.49	4.67	848.
2	10.65	21.26	4.22	5.50	720.
3	10.94	21.40	4.08	8.79	734.
4	10.40	20.98	4.09	1.86	25000.
5	11.28	20.66	3.64	4.07	15300.
6	12.26	19.70	1.65	6.52	14400.

---



---

**Table 2. Numerical Results for Model (5.2).**

---



---

Linear friction model (6.1)

iterate	$\alpha$	$\beta$	c	cost
0	12.00	20.00	35.00	301.
1	10.91	20.99	34.04	25.2
2	11.09	21.44	33.55	5.14
3	13.25	21.41	33.42	2.85
4	13.57	21.44	33.34	2.60
5	13.39	21.01	32.67	2.59

Quadratic friction model (6.2)

iterate	$\alpha$	$\beta$	$c_1$	$c_2$	cost
0	12.00	20.00	35.00	0.00	301.
1	11.01	20.85	34.19	-0.72	14.8
4	14.19	21.93	32.87	1.08	2.26
7	18.74	25.20	27.19	10.59	0.89
14	20.23	26.17	24.07	14.81	0.66

Piecewise linear friction model (6.3)

iterate	$\alpha$	$\beta$	$c_1$	$c_2$	cost
0	12.00	20.00	35.00	35.00	301.
1	11.27	20.70	34.30	35.70	5.00
2	11.31	20.91	34.20	35.68	0.21
3	11.81	21.09	34.21	35.49	0.116
4	12.05	21.42	34.72	36.00	0.112

---



---

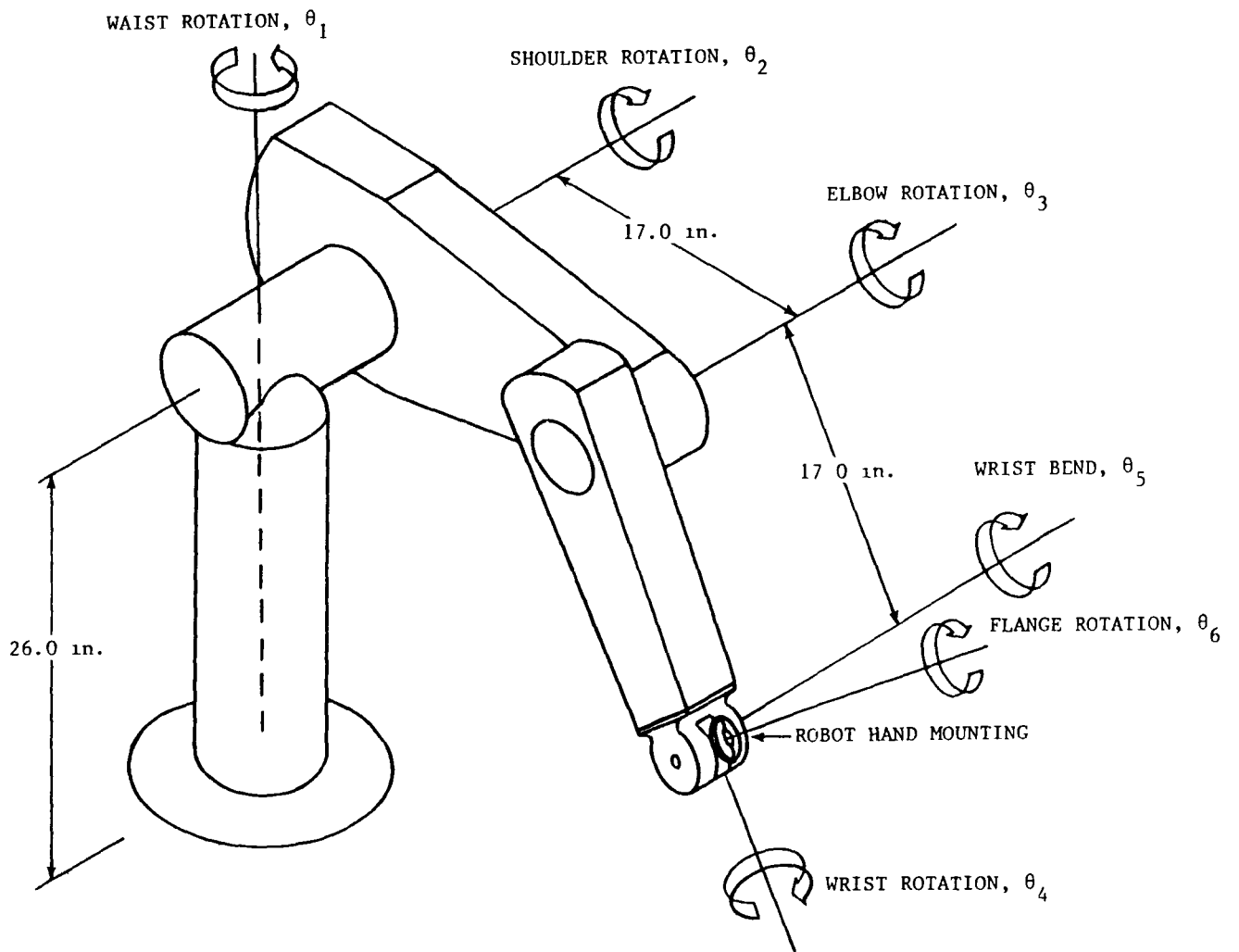


Figure 1. Robot arm with rotational joints [1].



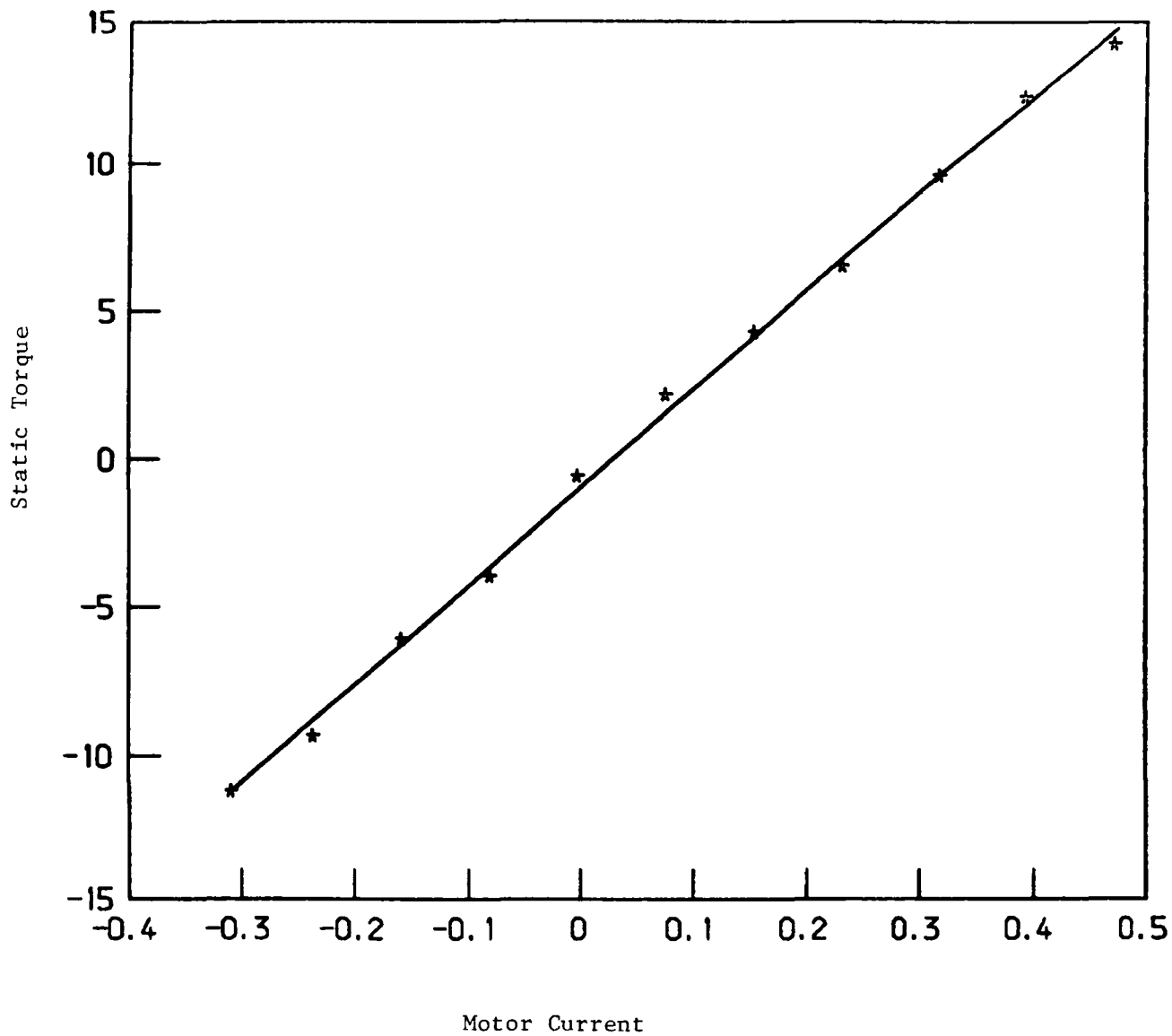


Figure 2. Static torque regression. Correlation coefficient is 0.999.

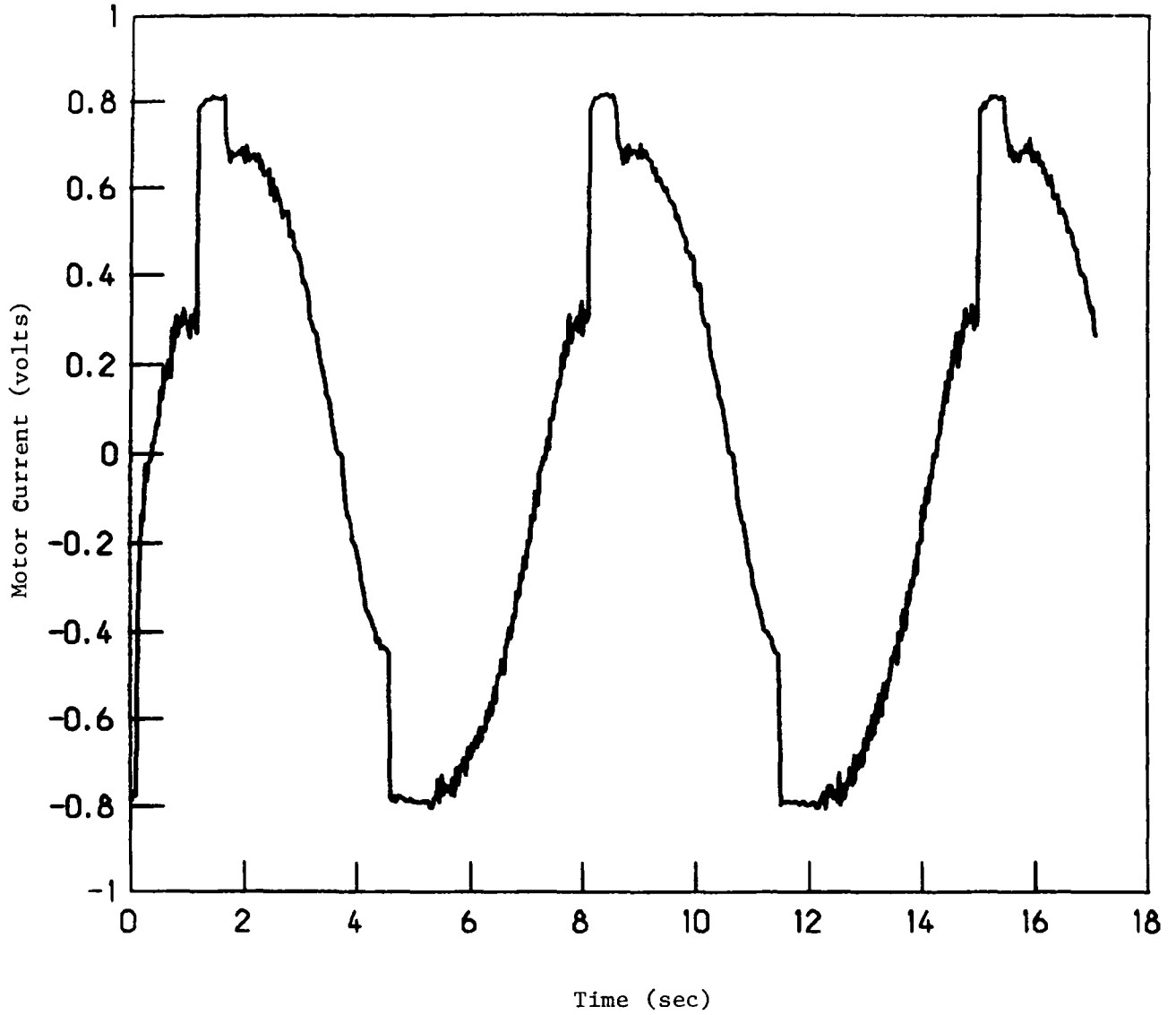


Figure 3. Input. The motor current was measured by the voltage drop across a known resistance.

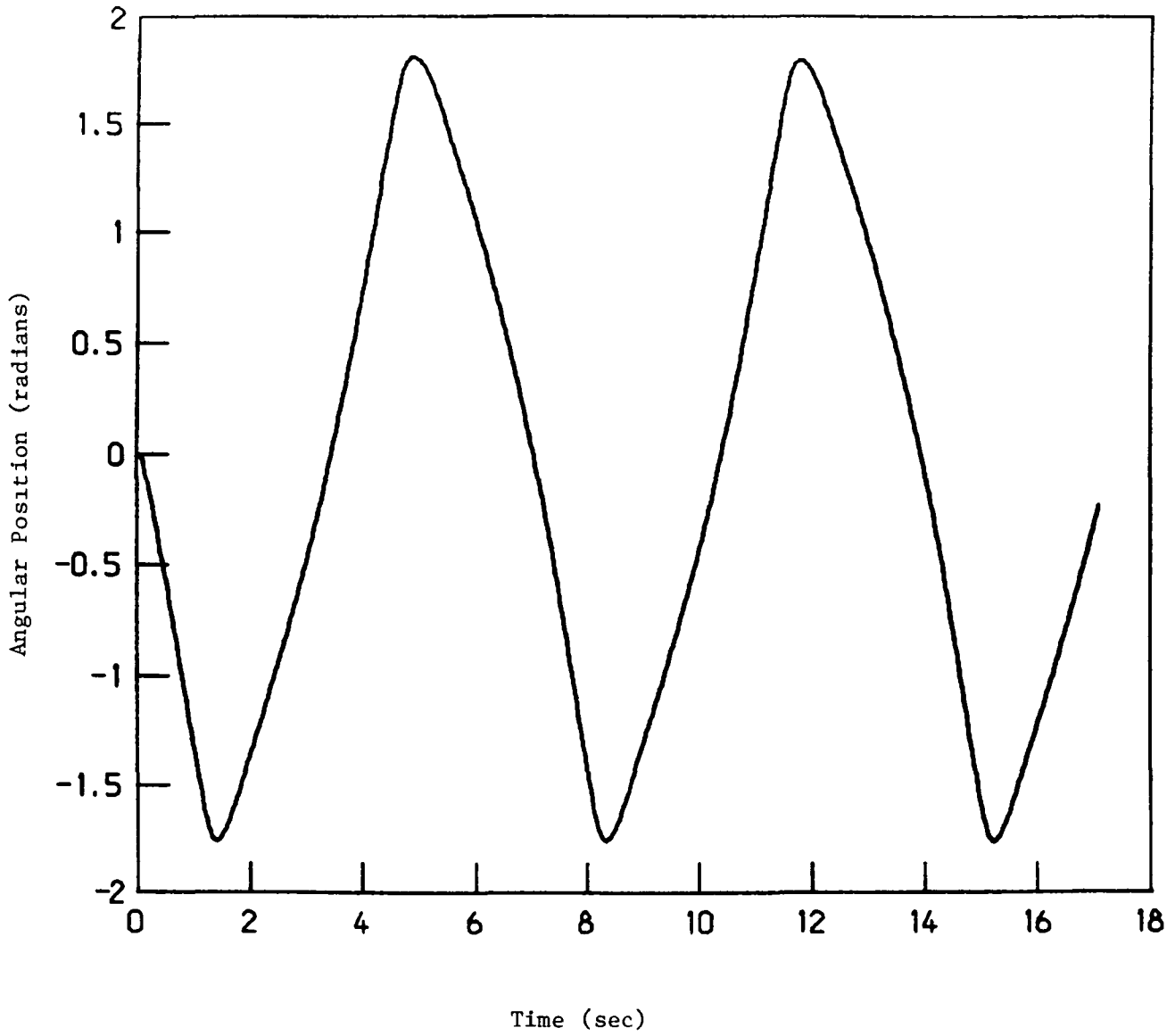


Figure 4. Output.

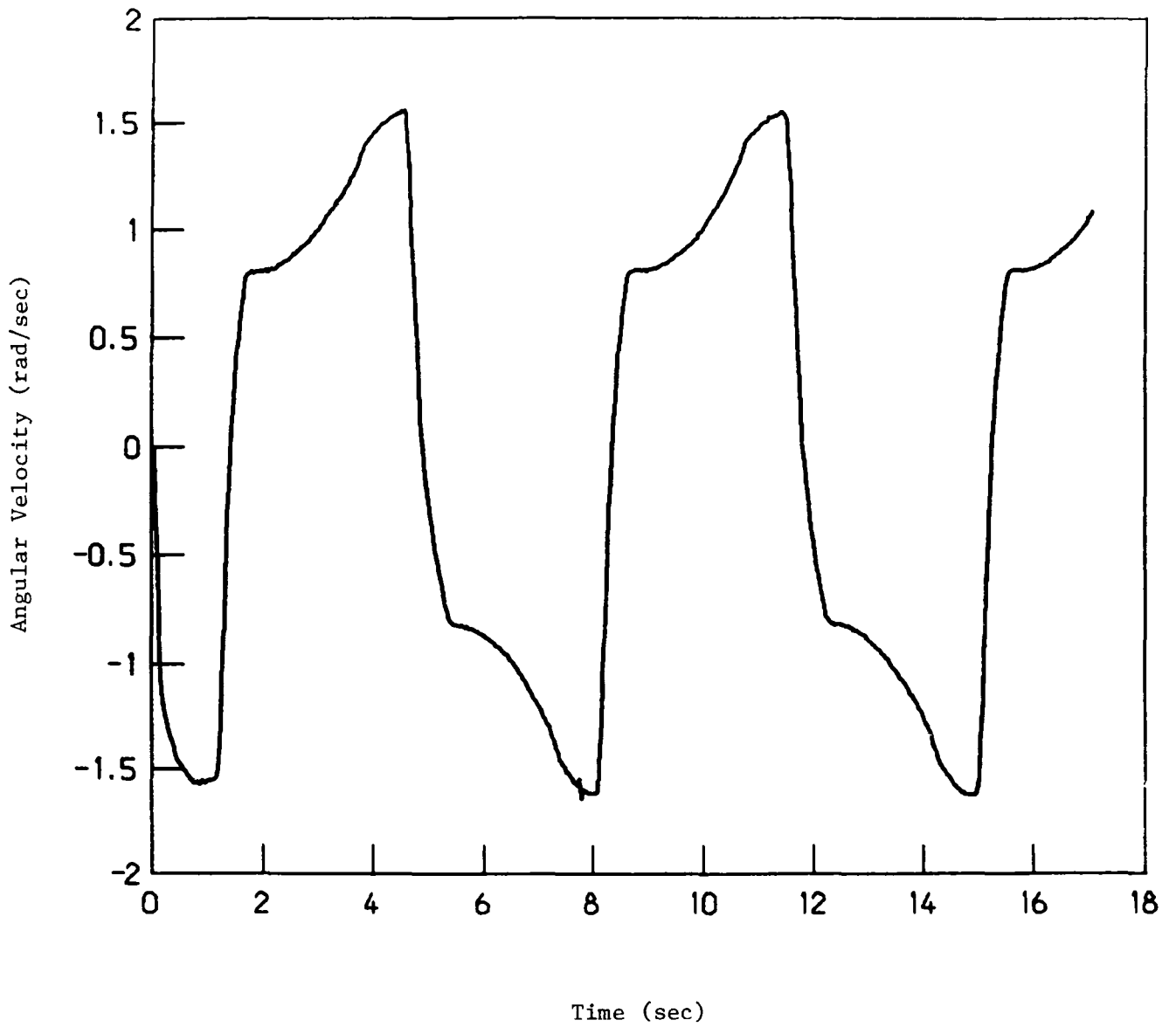


Figure 5. Differentiated output.

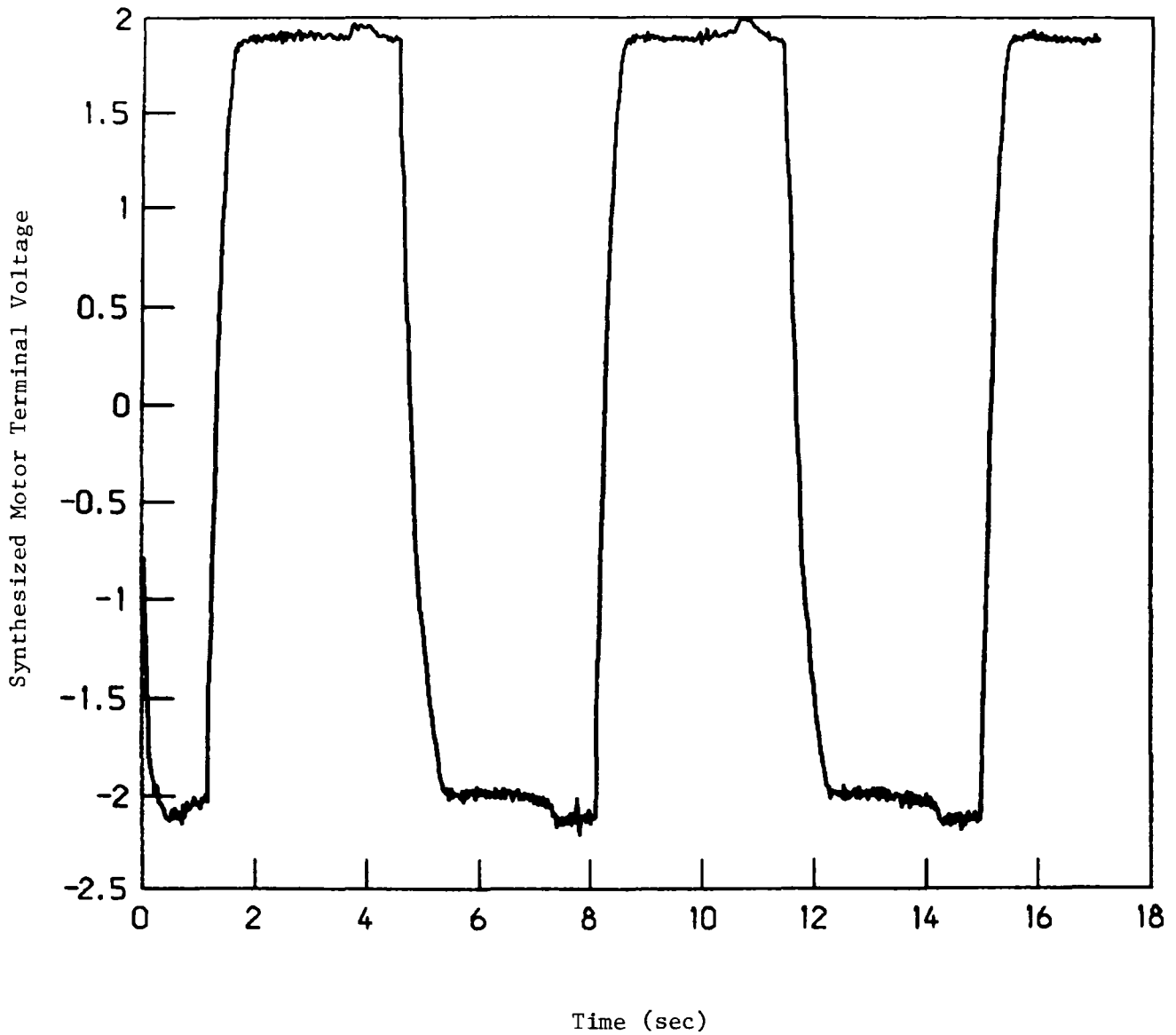


Figure 6. Synthesized input. This graph is the sum of Figure 3 and 1.5 times Figure 5.

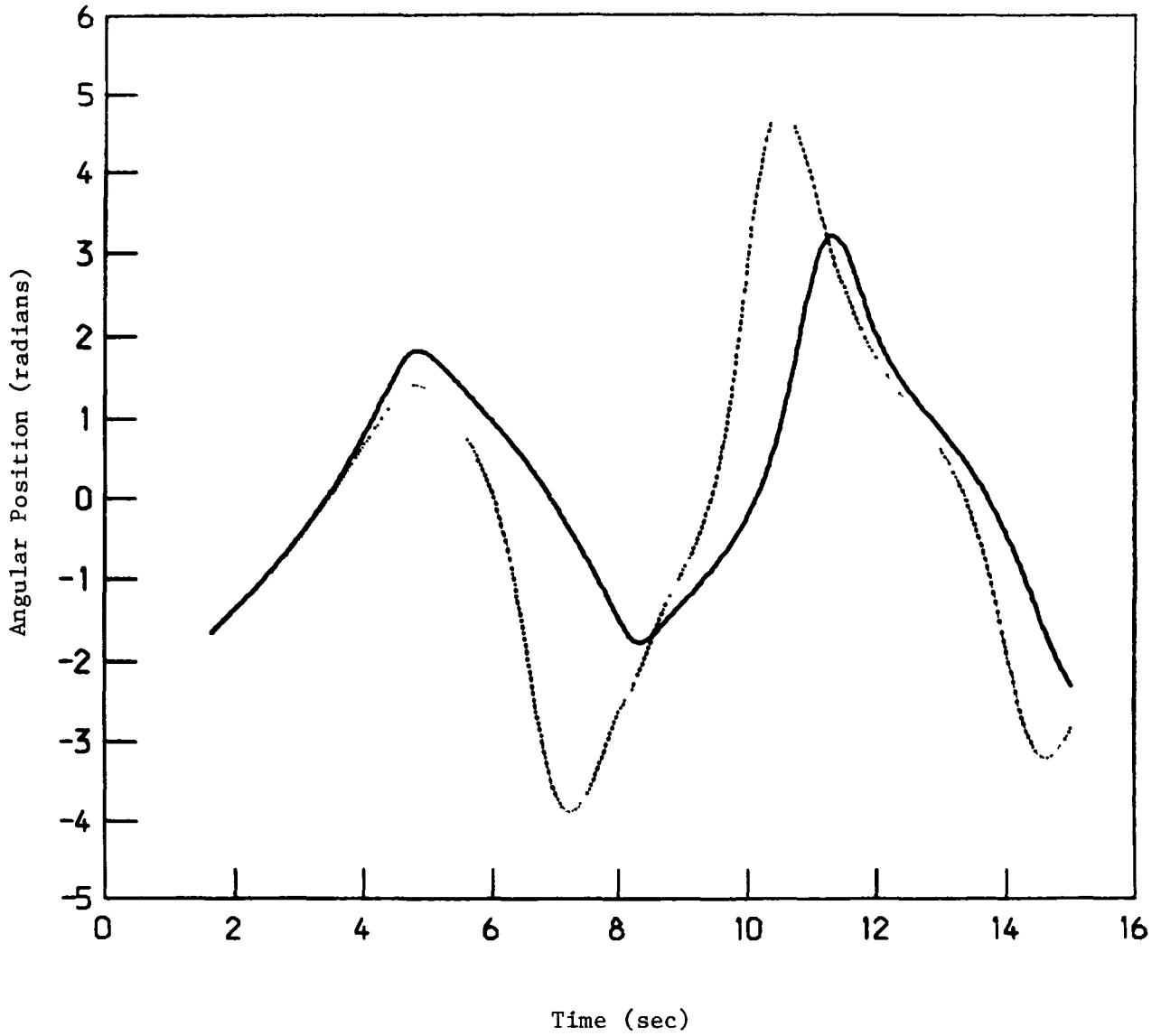


Figure 7. Parameter sensitivity for model (5.1) with friction model (6.3). Common parameters are  $\alpha = 12.74$ ,  $\beta = 21.209$ , and  $c_2 = 4.301$ . The perturbed parameter is  $c_1$  with  $c_1 = 2.296$  in the solid graph and  $c_1 = 2.306$  in the dotted graph.

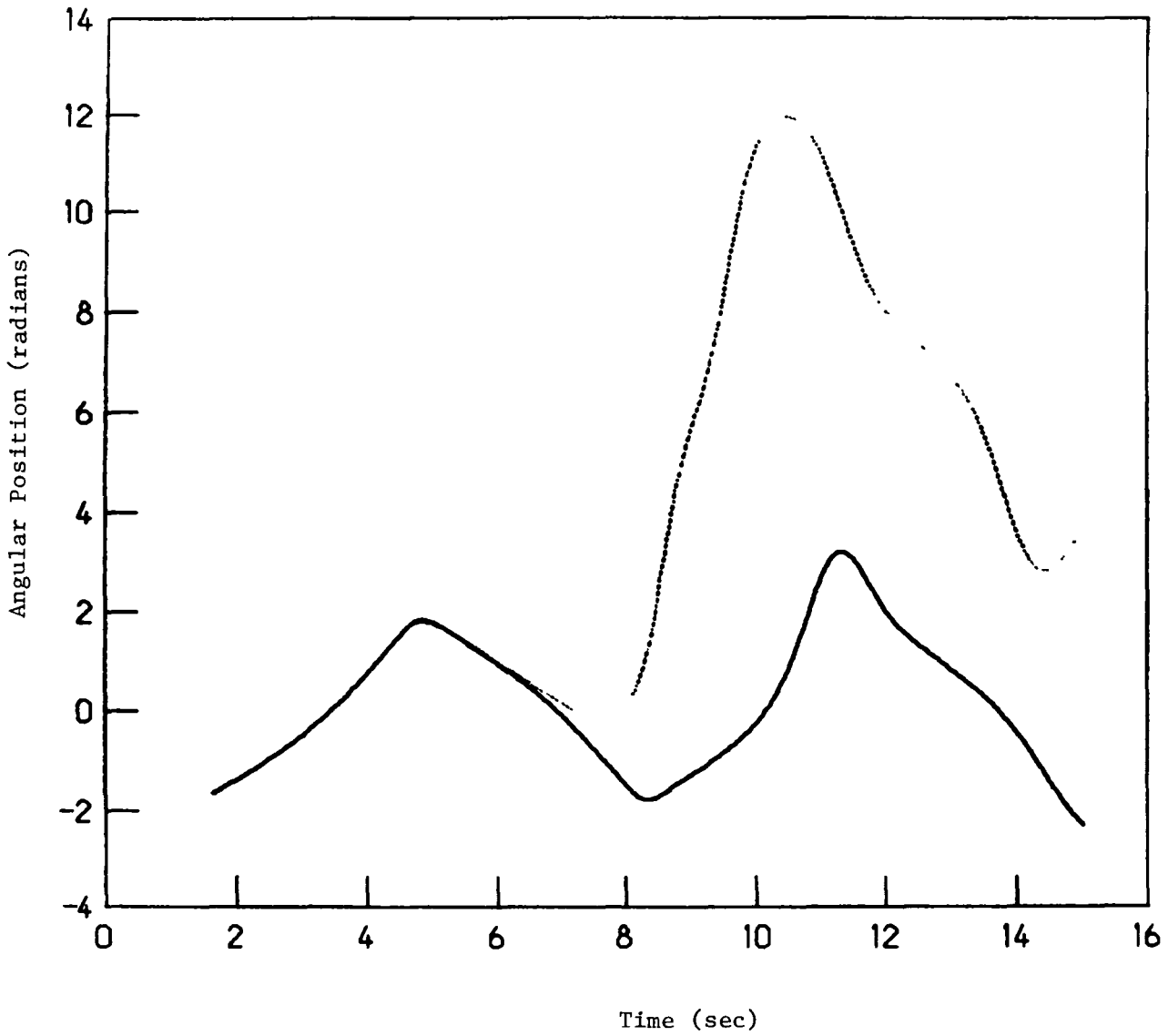


Figure 8. Initial angular velocity sensitivity for model (5.1) with friction model (6.3). Parameters are  $\alpha = 12.74$ ,  $\beta = 21.209$ ,  $c_1 = 2.296$ , and  $c_2 = 4.301$ . The angular velocity is  $\omega_0 = 0.63$  in the solid graph and  $\omega_0 = 0.64$  in the dotted graph.

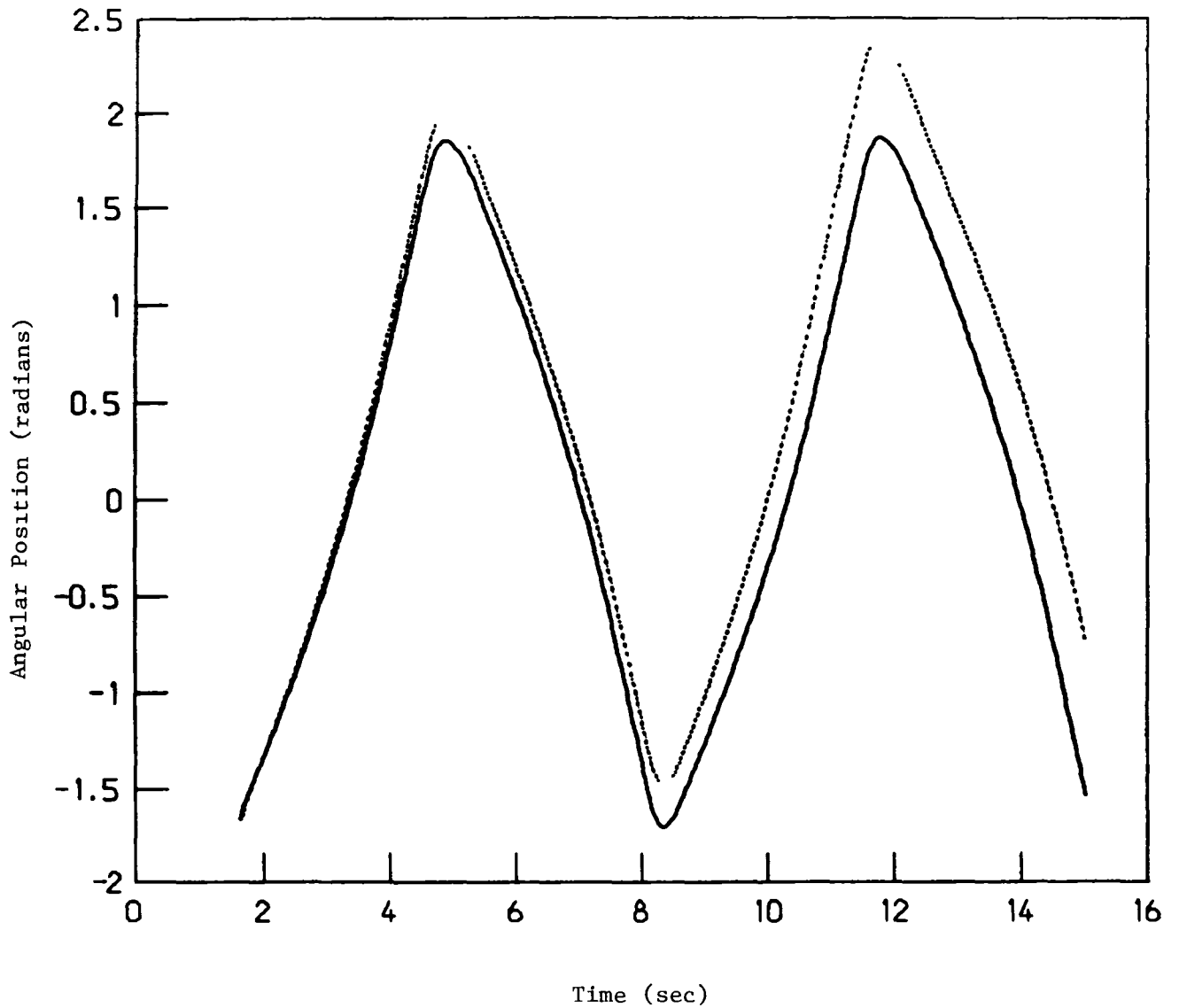


Figure 9. Parameter sensitivity for model (5.2) with friction model (6.3). Common parameters are  $\alpha = 12.05$ ,  $\beta = 21.42$ , and  $c_2 = 36.00$ . The perturbed parameter is  $c_1$  with  $c_1 = 34.72$  in the solid graph and  $c_1 = 33.72$  in the dotted graph.



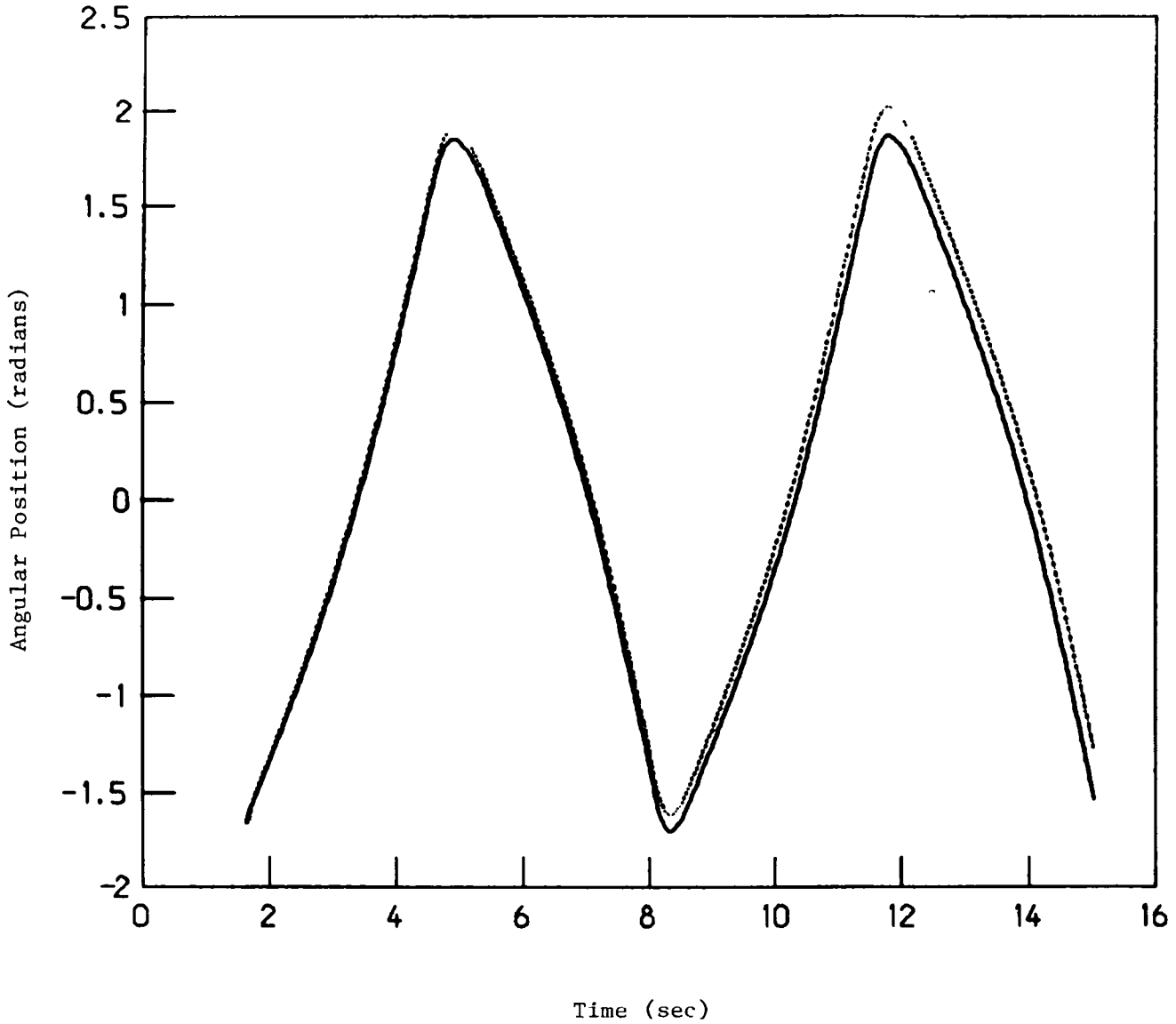


Figure 10. Initial angular velocity sensitivity for model (5.2) with friction model (6.3). Parameters are  $\alpha = 12.05$ ,  $\beta = 21.42$ , and  $c_1 = 34.72$ , and  $c_2 = 36.00$ . The initial angular velocity is  $\omega_0 = 0.76$  in the solid graph and  $\omega_0 = 1.76$  in the dotted graph.

1 Report No NASA CR-178002 ICASE Report No. 85-42		2 Government Accession No		3 Recipient's Catalog No	
4 Title and Subtitle PARAMETER IDENTIFICATION FOR A ROBOTIC MANIPULATOR ARM				5 Report Date September 1985	
				6 Performing Organization Code	
7 Author(s) D. W. Brewer and J. S. Gibson				8 Performing Organization Report No 85-42	
9 Performing Organization Name and Address Institute for Computer Applications in Science and Engineering Mail Stop 132C, NASA Langley Research Center Hampton, VA 23665				10 Work Unit No	
				11 Contract or Grant No NAS1-17070	
				13 Type of Report and Period Covered Contractor Report	
12 Sponsoring Agency Name and Address National Aeronautics and Space Administration Washington, D.C. 20546				14 Sponsoring Agency Code 505-31-83-01	
15 Supplementary Notes Langley Technical Monitor: J. C. South Jr. Submitted to Intl. J. Robotics Final Report					
16 Abstract  This paper describes the development of a nonlinear dynamic model for large oscillations of a robotic manipulator arm about a single joint. Optimization routines are formulated and implemented for the identification of electrical and physical parameters from dynamic data taken from an industrial robot arm. Special attention is given to the role of sensitivity in the formulation of robust models of this motion. The importance of actuator effects in the reduction of sensitivity is established and used to develop an electro-mechanical model of the manipulator system.					
17 Key Words (Suggested by Author(s))  robotic manipulator arm, identification sensitivity			18 Distribution Statement  64 - Numerical Analysis 66 - Systems Analysis Unclassified - Unlimited		
19 Security Classif (of this report) Unclassified		20 Security Classif (of this page) Unclassified		21 No of Pages 25	22 Price A02

**End of Document**